

Cite this: *RSC Advances*, 2011, 1, 474–483

www.rsc.org/advances

PAPER

## Rhodium catalyzed hydrogenation reactions in aqueous micellar systems as green solvents

M. Schwarze,<sup>a</sup> J.S. Milano-Brusco,<sup>a</sup> V. Stempel,<sup>a</sup> T. Hamerla,<sup>a</sup> S. Wille,<sup>b</sup> C. Fischer,<sup>c</sup> W. Baumann,<sup>c</sup> W. Arlt<sup>b</sup> and R. Schomäcker<sup>\*a</sup>

Received 1st July 2011, Accepted 5th July 2011

DOI: 10.1039/c1ra00397f

The hydrogenation of itaconic acid and dimethyl itaconate is transferred from methanol to aqueous micellar solutions of several surfactants, *e.g.*, SDS and Triton X-100, in order to facilitate the recovery of the catalyst. The reaction rate and selectivity strongly depends on the chosen surfactant and in some cases also on the surfactant concentration. In the best case the selectivity is the same as in methanol but the reaction rate is still lower because of a lower hydrogen solubility in water. Repetitive semi-batch experiments are chosen to demonstrate that high turn-over-numbers (>1000) can be reached in aqueous micellar solutions. No notable catalyst deactivation is observed in these experiments. The performance of micellar reaction systems is controlled by the partition coefficient of the substrates between the micelles and the continuous aqueous phase which can be predicted using the Conductor-like Screening Model for Real Solvents (COSMO-RS).

### 1. Introduction

Asymmetric homogeneous hydrogenation is a powerful tool in the synthesis of fine chemicals<sup>1</sup> and pharmaceuticals.<sup>2</sup> Well known examples are the rhodium catalyzed synthesis of L-Dopa<sup>3</sup> which is a pharmaceutical against parkinsonism, but meanwhile produced by using enzymes, and the iridium catalyzed synthesis of (*S*)-Metolachlor<sup>4</sup> which is used as a herbicide. In the last example, which is one of the most powerful asymmetric hydrogenation processes, a high turn-over-number (TON) combined with a high selectivity is reached in a batchwise process. Not every substrate-catalyst combination is able to reach an aspired high turn-over-number in one single batch run and therefore the catalyst has to be reused in order to obtain an acceptable cost efficient turn-over-number. Due to the fact that homogeneously catalyzed reactions usually are carried out in organic solvents like methanol or ethanol to ensure a good solubility of both, the substrate and the catalyst, separation of the catalyst from the reaction mixture is not a simple process and one major problem in comparison to heterogeneous catalysis. Commonly used separation techniques are distillation, chromatography or extraction and they are usually accompanied by catalyst deactivation because of thermal stress or loss of catalyst.<sup>5,6</sup> The heterogenization of homogeneous catalysts can overcome these problems and combine the advantage of high selectivity (homogeneous catalysis) with the advantage of simple separation (heterogeneous

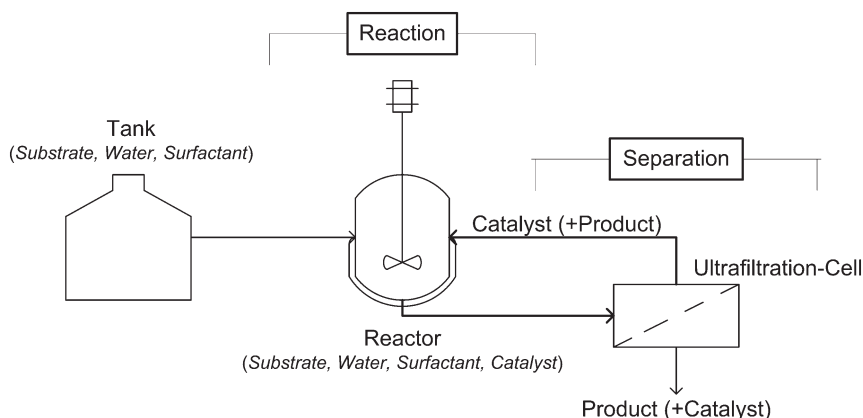
catalysis). Some examples for heterogenizations are (i) classical two-phase systems<sup>7</sup> (ii) ionic-liquids<sup>8–10</sup> (iii) supercritical fluids<sup>11</sup> and (iv) polymer supports.<sup>12,13</sup> In the last years the design of “greener”, “more sustainable” products and processes has become of great importance.<sup>14</sup> According to the guidelines of “Green Chemistry” water is a preferred solvent for chemical reactions because it is non-flammable and non-toxic. Unfortunately a lot of reactants and commonly used rhodium catalysts are hardly soluble in water and therefore reaction rates are very low. But a substantial acceleration of the reaction can be induced by adding surfactants. At surfactant concentrations higher than the critical micelle concentration (cmc) the surfactant monomers form aggregates, the micelles. The micelles consist of hydrophobic cores, able to solubilize hydrophobic reactants and homogeneous catalysts and a hydrophilic outer region. Therefore, the higher reaction rate in comparison to pure water can be explained by a higher local concentration of reactants inside the micelles. As already shown by Oehme,<sup>15</sup> Strukul<sup>16,17</sup> and other groups,<sup>18,19</sup> different type of reactions (*e.g.*, hydrogenations, hydroformylations or C–C coupling reactions) can be transferred from organic solvents to water this way. Together with the opportunity to perform reactions in water, the recyclability of the micellar embedded catalyst is given using micellar enhanced ultrafiltration.<sup>20,21,22</sup> A scheme for a continuous hydrogenation process using a micellar reaction medium, which can be divided into a reaction and a separation part, is shown in Scheme 1.

In the present study we demonstrate the feasibility of the application of aqueous micellar solutions with the example of a rhodium catalyzed homogenous hydrogenation of prochiral C–C double bonds in itaconates, *e.g.*, in dimethyl itaconate, mainly in

<sup>a</sup>Technical University of Berlin, Department of Chemistry, Straße des 17. Juni 124, 10623 Berlin, Germany

<sup>b</sup>Friedrich-Alexander-University Erlangen-Nürnberg, Chair of Separation Science and Technology, Egerlandstr.3, 91058 Erlangen, Germany

<sup>c</sup>Catalysis, Albert-Einstein Straße 29a, 18059 Rostock, Germany



**Scheme 1** Scheme of a reaction and catalyst recycling process using aqueous micellar solutions.

micellar solutions of sodium dodecyl sulfate (SDS) and Triton X-100 (TX-100). Dimethyl itaconate and itaconic acid are typical test substrates used to study enantioselective hydrogenation reactions.<sup>23,24</sup> Reaction rate and selectivity are compared with the results obtained from methanol as reference. Furthermore a suitable composition of a reaction medium for a continuous process will be formulated among others based on COSMO-RS (a quantum chemistry based a priori method to predict thermophysical data, see chapter 2.2) predictions of partition coefficients of reactants and products.

## 2. Methods

### 2.1 Experimental

**2.1.1 Chemicals.** For the experiments the following chemicals were used without further purification: itaconic acid (IA, Aldrich >99%), dimethyl itaconate (DMI, Fluka  $\geq 97\%$ ), diethyl itaconate (DEI, TCI >98%), dibutyl itaconate (DBI, TCI >95%), methanol (MeOH, Roth HPLC grade), chloroform (Acros HPLC grade), Triton X-100 (Sigma-Aldrich), sodium dodecyl sulfate ultrapure (SDS, AppliChem 99.5%), bis(1,5-cyclooctadiene)rhodium(I) trifluoromethane-sulfonate ( $\text{Rh}(\text{cod})_2\text{CF}_3\text{SO}_3$ , Strem 99%), (2*S*,4*S*)-1-tert-butoxycarbonyl-4-diphenylphosphino-2-(diphenylphosphinomethyl)-pyrrolidine (BPPM, Fluka >96%), (+)-1,1'-Bis((2*R*,4*R*)-2,4-diethylphosphotano)ferrocene(1,5-cyclooctadiene)rhodium(I)tetrafluoroborate ((*R,R*)-Et-FerroTane-Rhodium, Strem  $\geq 98\%$ ), Trimethylsilyldiazomethane (Sigma-Aldrich) and hydrogen (Messer-Griesheim 5.0). Additional surfactants (Dehyton K (29–32%), Dehypon LS 54 (>99.5%), Crafol AP 60 and Glucocon UP 215 (62–65%)) were received as a donation (Cognis, Germany) and the quality is given in the brackets. The difference to 100% is water.

**2.1.2 Determination of the critical micelle concentration (cmc).** Surface tension measurements of surfactant solutions were

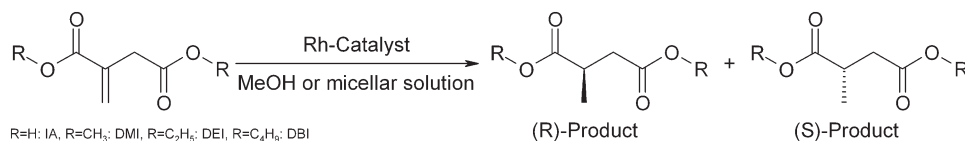
carried out in a DCAT 11 tensiometer from Dataphysics using the Du Noüy ring method with ring correction according to Huh & Mason. A standard solution of the surfactant was automatically mixed stepwise with bidistilled water and from the surface tension determined at 25 °C the cmc of the surfactant was calculated by the integrated software module.

**2.1.3 Determination of the micelle size.** For the determination of the micelle size dynamic light scattering (DLS) experiments were performed. The setup consisted of a 1 W Nd:YAG laser (Compass 150, Coherent, USA) and an ALV 5000/E autocorrelator (ALV, Germany). The analysis of the recorded correlation functions was done by the cumulant method.

**2.1.4 Hydrogenation procedure.** The reactions studied in this contribution are the asymmetric hydrogenations of itaconates catalyzed by Rh/BPPM or (*R,R*)-Et-FerroTane-Rhodium as shown in Scheme 2.

For the hydrogenation runs a thermostated 200 ml double wall glass reactor equipped with a gas dispersion stirrer was used. Semi-batch reactions were performed under a constant pressure of 0.11 MPa. The rate of hydrogen consumption [ $\text{dV}(\text{H}_2)/\text{dt}$ , mL/min] for keeping the pressure at a constant level and additionally the total amount of hydrogen [ $V_T$ , mL] were monitored.<sup>25</sup>

For all reactions at first the solvents (water, methanol) were purged in a separate flask with nitrogen for at least 60 min. Then the required compounds were added to the reactor in the following order: 95 mL water or MeOH, the surfactant, the substrate and 5 ml MeOH containing the catalyst. The catalyst Rh/BPPM was prepared *in situ* from 30 mg (0.064 mmol)  $\text{Rh}(\text{cod})_2\text{CF}_3\text{SO}_3$  and 39 mg (0.070 mmol) 2*S*,4*S*-BPPM while (*R,R*)-Et-FerroTane-Rhodium (10/20 mg, 13.7/27.0 mmol) was used as received. We used an excess of 10 mole-% BPPM to ensure the formation of the Rh/BPPM complex. After each addition the reactor was evacuated and refilled with nitrogen



**Scheme 2** Hydrogenation reaction of itaconates.

3 times. The mixture was heated up to the reaction temperature of 30 °C and stirred for 45 min at 400 min<sup>-1</sup>. The stirrer was stopped and the reaction was initiated after evacuating the reactor, followed by increasing the pressure to 0.11 MPa with hydrogen gas and restarting the stirrer at 800 min<sup>-1</sup>. When dV(H<sub>2</sub>)/dt was zero and V<sub>T</sub> became constant the reaction was finished. For IA and DMI the conversion (X<sub>E</sub>) and the enantiomeric excess (ee) after reaction were obtained using a gas chromatograph 5890 (Hewlett-Packard) with a chiral Lipodex E column (ca. 25 m, d = 0.25 mm, 0.6 bar N<sub>2</sub>, 90 °C, FID) from Macherey-Nagel. For the sample preparation at the end of the reaction a small amount of the aqueous micellar solution was taken and extracted with chloroform. For the hydrogenation of DMI, the extracted sample was directly injected into the GC while for the hydrogenation of IA the product was first transformed into the methylester using trimethylsilyldiazomethane. In case of DEI (T<sub>GC</sub> = 120 °C) and DBI (T<sub>GC</sub> = 150 °C) only the conversion was determined. With X<sub>E</sub> the conversion X(t) during reaction was calculated according to eqn (1).

$$X(t) = \frac{V(t)}{V_{total}} \cdot X_E \quad (1)$$

To compare the different reaction media the turn-over-frequency (TOF) was calculated.

**2.1.5 NMR studies.** 5.8 mg (0.009 mmol) [Rh((S,S)-MeDuPhos)(COD)]BF<sub>4</sub> were dissolved in 0.7 ml deuterated MeOH in a Young-NMR tube and were hydrogenated 1 h to generate the solvate complex. Under protective conditions 0.2 ml of Triton X-100 was transferred in the NMR tube. The measurements were carried out in a Bruker AV-400 spectrometer (frequency 400 MHz, magnetic field strength 9.4 T) at 297–298 K. For calibration of the <sup>31</sup>P-signals, 85% H<sub>3</sub>PO<sub>4</sub> were used as an external standard. The <sup>103</sup>Rh-NMR shifts were determined by <sup>31</sup>P, <sup>103</sup>Rh-HMQC measurements (with constant proton decoupling).<sup>26,27</sup> Every determination was carried out at least twice with different Rh-frequency offset and t1-increments to exclude folds of the signals along F1. The reference frequency were calculated with Ξ(<sup>103</sup>Rh) = 3.16 MHz. The evaluation and graphic processing of the measuring data occurred with the software *Bruker NMR-TopSpin 1.3*.

## 2.2 Modeling

In this study the Conductor-like Screening Model for Real Solvents (COSMO-RS) is used to predict partition coefficients of reactants and products in micellar solutions. The model has already shown its potential to predict partition coefficients in micellar systems a priori.<sup>28</sup> An a priori prediction is possible, since thermodynamic properties such as activity coefficients are calculated based only on the molecular structure.<sup>29</sup> In the COSMO-model the solvent is treated as embedded in a conductor of dielectric constant infinity. The dipoles on the surface of the molecule influence the electron density and its structural parameters of the molecule. COSMO can differ between conformers, *i.e.* isomers which can be differed by its quantum chemical energy. The set of conformers used for the calculation has a remarkable influence<sup>28</sup> on the result. The transfer from the state of the molecule embedded into a virtual

conductor to a real solvent is done by applying the COSMO-RS concept which applies statistical thermodynamics to charge segments on the surface of the pure molecule (“sigma profile”). Mixtures are represented by comparing the sigma-profiles of different molecules. If the profiles add to zero (no charge left, activity coefficient equals 1), the compounds form an ideal solution. All deviations are called “misfit” and represent the non-ideality of the mixture (activity coefficients different from 1 but positive). In the present study the conformational search for all solutes (itaconic acid and its derivatives) and the ionic surfactants sodium dodecyl sulfate (SDS) was performed *via* molecular mechanics using the force field MM+ in the program HyperChem. The conformer set of the nonionic surfactant Triton X-100 was additionally optimized by molecular dynamic simulation.<sup>28</sup> All those conformers were further optimized by using the software Turbomole® to perform the DFT calculation (Version 5.7. and 5.10). The activity coefficients of the solutes are then calculated using the COSMOtherm program [F. Eckert and A. Klamt, COSMOtherm, Version C2.1, Release 01.04; COSMOlogic GmbH & Co. KG, Leverkusen, Germany, 2004]. Herein the activity coefficient γ<sub>i</sub> of component i can be written as:

$$\gamma_i = \exp\left(\frac{\mu_i^* - \mu_i^0}{RT}\right) \quad (2)$$

whereas μ<sub>i</sub><sup>\*</sup> = μ<sub>i</sub> - RTlnx<sub>i</sub>, μ<sub>i</sub> and μ<sub>i</sub><sup>\*</sup> are the chemical potentials of component i in the mixture and in the reference state of pure liquid, correspondingly.

When using the COSMO-RS model to predict partition coefficients in micellar systems, the pseudo-phase approach is used. The partition coefficient of a solute is calculated based on the thermodynamic equilibrium conditions as follows:

$$K^{MW} = \frac{x_i^{\text{micellar phase}}}{x_i^{\text{aqueous phase}}} = \frac{\gamma_i^{\text{aqueous phase}}}{\gamma_i^{\text{micellar phase}}}; \quad x_i \rightarrow 0 \quad (3)$$

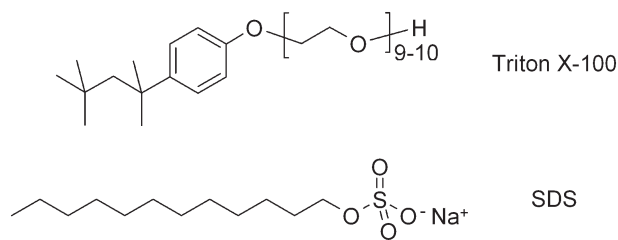
Where x<sub>i</sub><sup>micellar phase</sup> and x<sub>i</sub><sup>aqueous phase</sup> are the mole fractions of solute i in the surfactant and aqueous phases and γ<sub>i</sub><sup>micellar phase</sup> and γ<sub>i</sub><sup>aqueous phase</sup> are the activity coefficients of solute i in the surfactant and the aqueous phase, respectively. The power of the COSMO-RS approach is that the partition coefficient of any structure of the surfactant can be predicted, thus tailoring the surfactants to the aim of the chemical reaction and the subsequent separation simultaneously.

## 3. Results and discussion

### 3.1 Characterization of the surfactants

From the pool of available surfactants we selected SDS and TX-100 for our investigations. These surfactants are frequently studied and commercially available with the same quality. Additionally, some other surfactants which were a donation from the company Cognis were tested in order to look for more sustainable surfactants. The structures of SDS and Triton X-100 are shown in Scheme 3. Further information like the cmc and the micelle diameter (d<sub>micelle</sub>) used to characterize aqueous-micellar solutions is given in Table 1.

For often investigated surfactants, characteristic surfactant data can be obtained from the literature, but to proof the quality



**Scheme 3** Structure of SDS and Triton X-100.

**Table 1** Micelle diameter and critical micelle concentration ( $T = 25\text{ }^{\circ}\text{C}$ ) for investigated surfactants

Surfactant	Type	cmc (g/L)	$R_{h, \text{Micelle}}$ (nm)	pH <sup>b</sup>
SDS	anionic	2.3, 2.3 <sup>30a</sup>	1.03	6.5–8
TX-100	non-ionic	0.33, 0.32 <sup>31</sup>	4.34, 4.4 <sup>32</sup>	6–8
Dehyton K	amphoter	0.009	2.9	11.0
Dehyton LS 54	non-ionic	0.0015	6.7	6.5
Crafol AP 60	unknown	0.685	11.1	0–2.5
Glucopon UP 215	non-ionic	0.4	3.3	11.9

<sup>a</sup> From conductivity measurements;  $R_h$ : hydrodynamic radius. <sup>b</sup> From customer information.

of the delivered substances that could change between different batches, own measurements are reasonable and were performed in this case. These data show that the micelle diameter is between 1–10 nm while the cmc is in the range of 0.1 mg/L–3 g/L. Generally ionic surfactants have higher cmc values and form smaller micelles than non-ionic surfactants. From this point of view non-ionic surfactants should be favored for hydrogenation reactions in aqueous micellar media because less material is needed and membrane separation should be easier. In the membrane separation process again the interaction of the reactants, essentially the catalysts with the micelles and the interaction of the reaction mixture with the membrane are also of great importance. Therefore a surfactant is required that will lead to the best performance with respect to both, reaction and separation.

### 3.2 Asymmetric hydrogenations

**3.2.1 Catalyst activation.** We used two chiral catalysts in our investigations. The first one was the in situ prepared Rh/BPPM catalyst which was successfully used several times for hydrogenations in micellar solutions.<sup>33,34</sup> The second one was a commercial catalyst named (*R,R*)-Ethyl-FerroTane-Rhodium, which was tested because it shows excellent performance in the hydrogenation of DMI in methanol.<sup>35</sup> Both catalysts are not fully active when starting the hydrogenation reaction and an activation period can be observed. This activation period is not unusual if the catalyst or the catalyst precursor contain cyclooctadiene (COD) ligands like in our case. The COD has to be hydrogenated first, before full activity is developed. The appearance of induction periods was already reported in literature.<sup>36</sup> For a detailed kinetic investigation the fully active catalyst complex is needed which can be obtained by a pre-hydrogenation of the catalyst (Fig. 1) before adding the substrate. We found that 60 min pre-hydrogenation time is adequate in order to reach optimal performance.

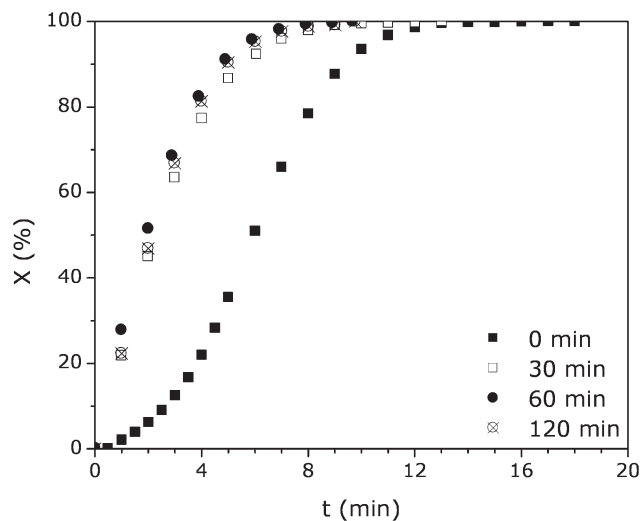


**Fig. 1** Conversion progress for the Rh/BPPM (64.1  $\mu\text{mol}$  Rh(cod)<sub>2</sub>-CF<sub>3</sub>SO<sub>3</sub>, 70.4  $\mu\text{mol}$  BPPM) catalyzed hydrogenation reaction of DMI (6.3 mmol) in methanol ( $V = 100\text{ mL}$ ) at different pre-hydrogenation times.

The activation of the catalyst can also be performed using one batch run prior to the desired experiment as shown in Fig. 2.

There are some rhodium catalysts, e. g., of the norbornadiene (NBD) type, that can overcome the problem of an induction period because NBD complexes are hydrogenated faster than COD complexes,<sup>37</sup> but it is unclear how these complexes will interact with the aqueous micellar solution. It is expected that rhodium/nbd complexes are much more sensitive than rhodium/cod complexes and unfavorable reaction media can lead to a fast deactivation of the catalyst.

**3.2.2 Hydrogenation in micellar solutions.** **3.2.2.1 Surfactant Screening.** The aim of this study was to find an aqueous micellar solution that can be used as an alternative reaction medium to replace polar organic solvents. An appropriate surfactant that

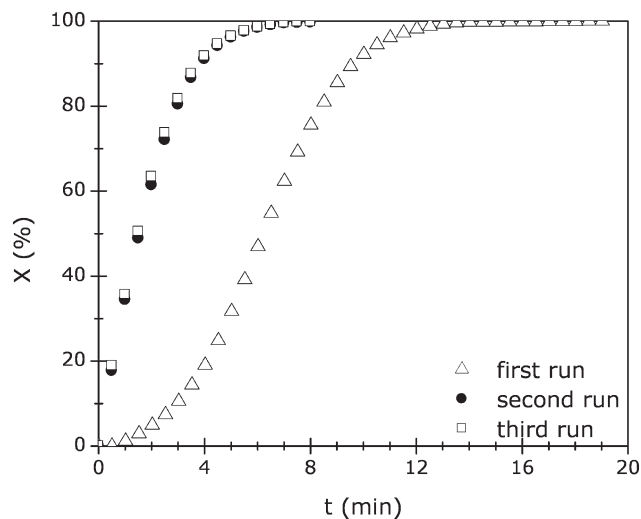


**Fig. 2** Conversion progress for the Rh/BPPM (64.1  $\mu\text{mol}$  Rh(cod)<sub>2</sub>-CF<sub>3</sub>SO<sub>3</sub>, 70.4  $\mu\text{mol}$  BPPM) catalyzed hydrogenation reaction of DMI (6.3 mmol) in methanol ( $V = 100\text{--}103\text{ mL}$ ) in repetitive batch mode.

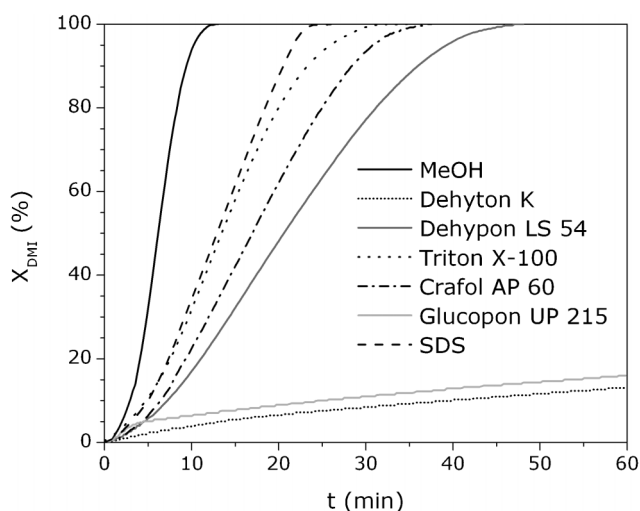


**Fig. 3** Conversion progress for the Rh/BPPM (64.1  $\mu\text{mol}$  Rh(cod)<sub>2</sub>-CF<sub>3</sub>SO<sub>3</sub>, 70.4  $\mu\text{mol}$  BPPM) catalyzed hydrogenation reaction of DMI (6.3 mmol, 12.6 mmol in SDS) in methanol ( $V = 100$  mL) and in different aqueous micellar solutions ( $V = 100$ – $105$  mL,  $c_{\text{surfactant}} = 12$ – $40$  g/L).

will lead to acceptable catalytic activity without loss of selectivity in the asymmetric hydrogenation in aqueous micellar solutions was searched for. The lower reactivity can later be compensated by the advantages in catalyst recovery by micellar enhanced ultrafiltration. Therefore, at first, all available surfactants were screened using the Rh/BPPM catalyzed hydrogenation of DMI as test reaction. As reference system we selected methanol. In Fig. 3 the reaction progress of the hydrogenation of DMI is shown for all investigated reaction media. The enantiomeric excesses are given in Table 2.

Substantial differences between the hydrogenation reactions of DMI in presence of different surfactants were encountered. The conversion varies from less than 20% within 60 min (Dehyton K, Glucopon UP 215) up to 100% within 20–30 min (SDS, Triton X-100), whereas by using methanol as reaction medium full conversion is reached within 10 min. It is not unexpected that the hydrogenation is faster in methanol because of a higher hydrogen solubility in methanol in comparison to water (Fig. 4).

Another difference in the reaction behavior can be seen in the different results for the enantiomeric excess. While the ee for the reference system is about 70% it varies from 25% (Dehyton K) to 69% (SDS) for the micellar solutions. In general the quality of many available surfactants is not 100% pure material. That means the surfactants show not negligible contaminations with associated materials (*e.g.* salts) that come from the production process. The interaction of the catalyst with the surfactant itself

**Table 2** Enantiomeric excess for the hydrogenation of DMI as shown in Fig. 3

Reaction solution	ee (%)
MeOH	71 S
H <sub>2</sub> O / SDS	69 S
H <sub>2</sub> O / Triton X-100	61 S
H <sub>2</sub> O / Dyhypon LS 54	60 S
H <sub>2</sub> O / Crafol AP 60	56 S
H <sub>2</sub> O / Glucopon UP 215	30 S
H <sub>2</sub> O / Dehyton K	25 S

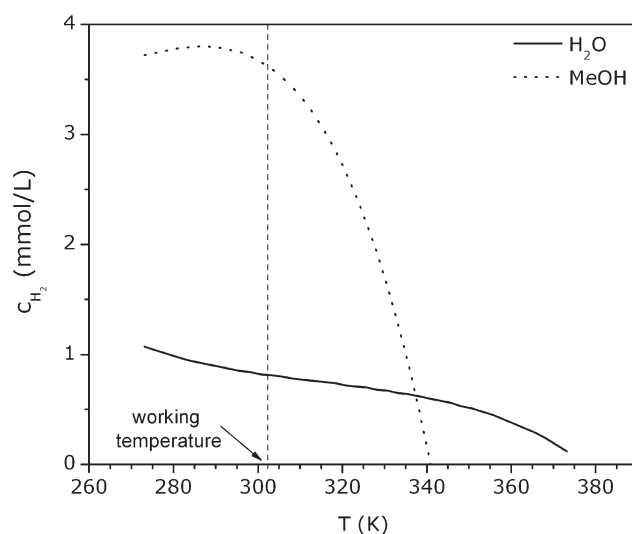


**Fig. 4** Calculated hydrogen concentration in water and methanol ( $p = 0.11$  MPa).<sup>38</sup>

and the associated material can be responsible for changes in the reaction rate and selectivity. Often traces of an incompatible compound are responsible for a deactivation of the catalyst. In this case the results seem to be related to the pH-value in solution. For the solutions of Dehyton K and Glucopon UP 215, which show high pH values, the reactions are slow and the ee's are low. For Crafol AP 60 that has a low pH value the ee is better but lower than for the surfactant systems with neutral pH. We tested the surfactants without further purification in order to find an appropriate aqueous surfactant solution for the hydrogenation of DMI without additional time and cost intensive purification steps. Therefore, the best results were achieved using SDS or Triton X-100 as surfactants.

**3.2.2.2 Hydrogenation in micellar solutions of SDS and Triton X-100.** The hydrogenation of high amounts of non- or less water-soluble substrates under homogeneous conditions is only possible when an appropriate amount of surfactant is added to the solution to solubilize the substrates. After determination of the required surfactant concentration the reaction behavior is very similar to methanol. In Table 3 results for the hydrogenation for different itaconates are given.

It shows that the reaction is always faster in methanol but the ee is the same. Rh/BPPM leads to better ee for IA hydrogenation than for DMI hydrogenation while for (*R,R*)-Et-FerroTane-Rhodium the reverse case is observed. In our investigation we found that (*R,R*)-Et-FerroTane-Rhodium is more sensitive to the surfactant systems than Rh/BPPM and therefore we used the later for the further studies. Furthermore we focused on the hydrogenation of DMI in order to demonstrate the influence of an aqueous micellar TX-100 solution (40 g/L) for an only weakly water soluble substrate. The TOF for the hydrogenation of DMI a function of substrate concentration is shown in Fig. 5.

With increasing substrate concentration the TOF increases up to a saturation value while the enantiomeric excess is constant at about 60% for the *S* enantiomer. The change in TOF can be explained assuming a Michaelis–Menten analogue kinetic model for the DMI hydrogenation. Therefore the velocity of the

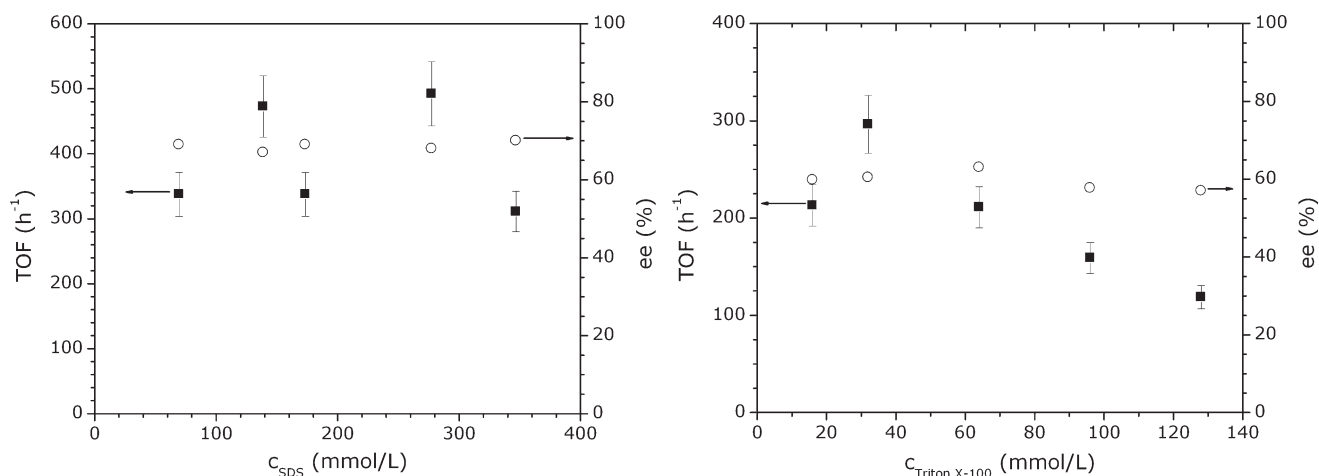
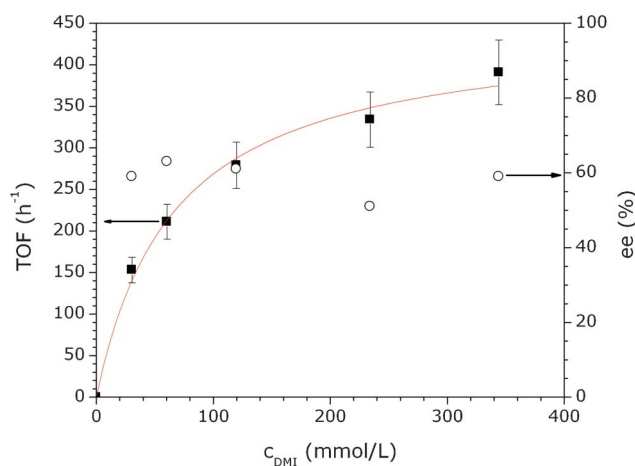
**Table 3** TOF and ee for the hydrogenation of itaconates ( $p = 0.11$  MPa,  $T = 30$  °C)

Entry	Catalyst	Substrate	[S]/[C]	Solution	TOF ( $\text{h}^{-1}$ )	ee (%)
1	Rh/BPPM	IA	1080/1	MeOH	5900	95 S
2	Rh/BPPM	IA	240/1	TX-100 (40 g/L)	480	>95 S
3	FerroTane	IA	1700/1	MeOH	7300	75 S
4	FerroTane	IA	280/1	SDS (100 g/L)	600	n. d.
5	FerroTane	IA	1700/1	SDS (50 g/L)	560 <sup>a</sup>	72 S
6	FerroTane	IA	1700/1	TX-100 (10 g/L)	600 <sup>a</sup>	70 S
7	Rh/BPPM	DMI	200/1	MeOH	740	71 S
8	Rh/BPPM	DMI	200/1	TX-100 (40 g/L)	260	61 S
9	Rh/BPPM	DMI	200/1	SDS (50 g/L)	340	69 S
10	FerroTane	DMI	470/1	MeOH	2800	95 S
11	FerroTane	DMI	470/1	TX-100 (40 g/L)	460 <sup>b</sup>	91 S
12	FerroTane	DMI	280/1	SDS (100 g/L)	670	91 S
13	FerroTane	DMI	470/1	SDS (50 g/L)	700	92 S
14	Rh/BPPM	DEI	80	MeOH	280	-
15	Rh/BPPM	DEI	80	TX-100 (40 g/L)	180	-
16	FerroTane	DEI	280	SDS (100 g/L)	500	-
17	Rh/BPPM	DBI	100	MeOH	350	-
18	FerroTane	DBI	290	SDS (100 g/L)	390	-

<sup>a</sup> Stopped after 1h at 35% conversion. <sup>b</sup> Conversion only 75%; n. d: not determined; Error for TOF:  $\pm 10\%$ .

reaction increases as long as the substrate concentration is below the saturation concentration and will be constant above. This dependency on the substrate concentration for DMI is also observed for the rhodium catalyzed hydrogenation of the other substrates.<sup>39</sup> The surfactant concentration is an important parameter which has to be taken in account when designing a process applying the aqueous micellar solutions as reaction media. In case of the catalyst recovery by micellar enhanced ultrafiltration the surfactant and an appropriate ultrafiltration membrane are responsible for the simultaneous product isolation and catalyst retention. For Triton X-100 and SDS the mean TOF as function of the surfactant concentration is shown in Fig. 6.

While in the case of SDS the TOF is scattering around a value of  $400 \text{ h}^{-1}$  for Triton X-100 the TOF decreases when the surfactant concentration is increased. The enantiomeric excess in both cases is constant at 69% (SDS) and 60% (Triton X-100), respectively. An explanation for the different behavior in the rate can be given by an analysis of the surfactant structure. The structure of Triton X-100

**Fig. 6** TOF and ee for the Rh/BPPM ( $64.1 \mu\text{mol Rh}(\text{cod})_2\text{CF}_3\text{SO}_3$ ,  $70.4 \mu\text{mol BPPM}$ ) catalyzed hydrogenation reaction of DMI at different surfactant concentrations in SDS ( $c_{\text{DMI}} = 126 \text{ mmol/L}$ ) and Triton X-100 ( $c_{\text{DMI}} = 63 \text{ mmol/L}$ ) solutions. Error for TOF:  $\pm 10\%$ .**Fig. 5** TOF and ee for the Rh/BPPM ( $64.1 \mu\text{mol Rh}(\text{cod})_2\text{CF}_3\text{SO}_3$ ,  $70.4 \mu\text{mol BPPM}$ ) catalyzed hydrogenation reaction of DMI at different substrate concentrations in aqueous micellar TX-100 solution (40 g/L,  $V=104\text{--}110 \text{ mL}$ ). Error for TOF:  $\pm 10\%$ .

includes an aromatic ring that forms a  $\eta^6$ -aromatic complex with rhodium. In the  $^{31}\text{P}$  NMR spectrum a broad doublet is observed at 97.3 ppm with a Rh-P coupling constant of 204 Hz. This is within the range of other  $\eta^6$ -arene complexes with the same phosphane, e.g.  $[\text{Rh}(\text{Me-DuPhos})(\text{toluene})]\text{BF}_4$  ( $^1J_{\text{P,Rh}} = 202 \text{ Hz}$ ) and  $[\text{Rh}(\text{Me-DuPhos})(\text{benzene})]\text{BF}_4$  ( $^1J_{\text{P,Rh}} = 201 \text{ Hz}$ ). Further unambiguous characterization comes from  $^1\text{H}$  NMR (coordinated arene shifted to lower frequencies: 7.17, 6.98, 6.37, and 6.05 ppm) and  $^{103}\text{Rh}$  NMR (Fig. 7) where a clear correlation signal is found with a chemical shift of  $-1006 \text{ ppm}$  which corresponds well to that of known arene complexes, as  $-1139 \text{ ppm}$  and  $-1162 \text{ ppm}$  for the above mentioned toluene and benzene complexes, respectively.

The formation of this type of complexes and an inhibition of the reaction was shown earlier using aromatic solvents in rhodium catalyzed hydrogenations.<sup>40</sup>

For the surfactants SDS and TX-100 the ee for the hydrogenation of DMI in aqueous-micellar solutions with Rh/BPPM is almost the same than in methanol, although the rates are lower and particular decreasing with surfactant concentration. From

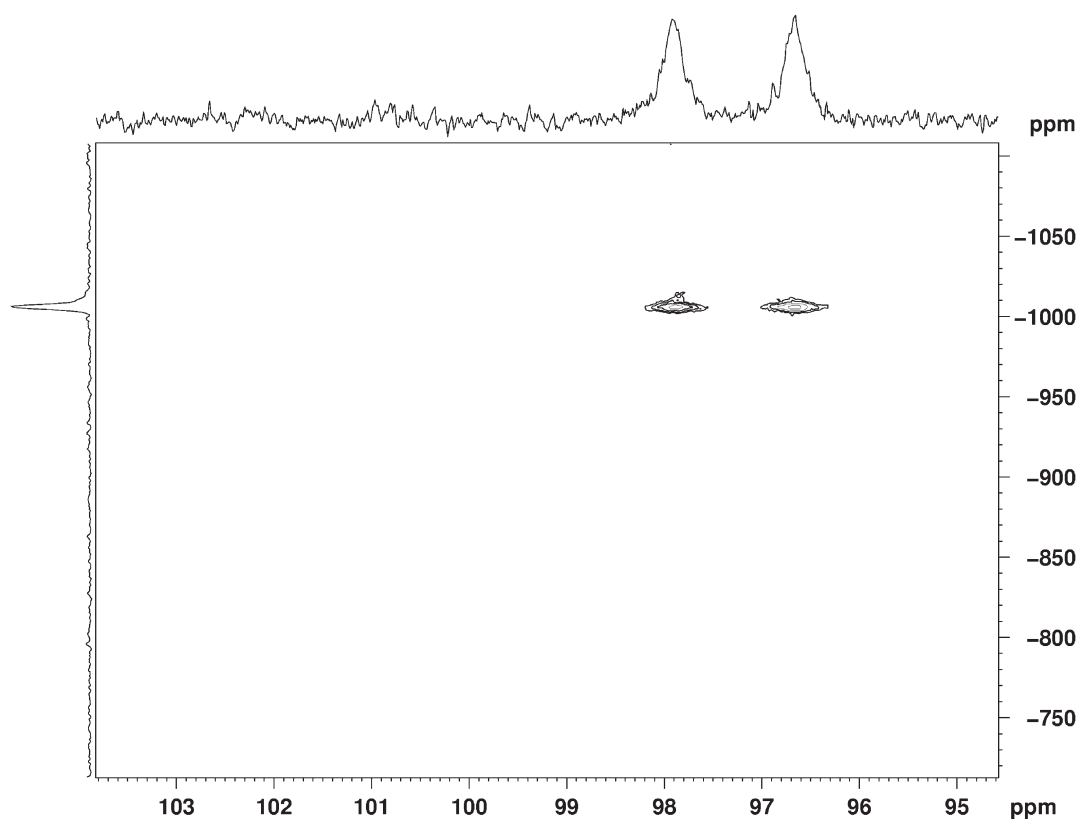


**Fig. 7**  $^{31}\text{P}, ^{103}\text{Rh}\{^1\text{H}\}$  HMQC NMR spectrum for  $[\text{Rh}((S,S)\text{-Me-DuPhos})(\text{Triton X-100})]\text{BF}_4$  in methanol- $d_4$ , taken at 317 K. The chemical shift  $\delta$  of the  $^{103}\text{Rh}$  NMR signal ( $-1006$  ppm) is within the range of known Rh-arene complexes.

reactions carried out in a pure homogenous environment, often lower selectivity is obtained in case of slow reaction rates. This behavior was also found in some of our investigations with the (*R,R*)-Et-FerroTane-Rhodium catalyst that shows very low ee values if the catalyst concentration is chosen to low, because then catalyst deactivation dominates during the reaction. For the Rh/BPPM catalyst, we assume a better compatibility with the micellar medium, because the ee values were more or less constant. Furthermore, based on the partition coefficient, the catalyst is embedded into the hydrophobic core of the micelles and thereby protected. As already mentioned, the reason for the low activity in water is only the lower hydrogen solubility in comparison to methanol.

**3.2.3 Catalyst stability.** The monitoring of a catalytic reaction beyond a standard batch run reveals additional information about the stability of the catalyst in such media. For the hydrogenation of DMI with Rh/BPPM in aqueous micellar solutions of Triton X-100 and SDS we added several times (3–6 times) the same amount of DMI and calculated the TOF for each run (Fig. 8).

The TON obtained after all runs is 380 for the TX-100 solution and 1250 for the SDS-solution. In both media the TOF is increasing from the first run to the second run because of the catalyst activation but then the TOF decreases continuously, while in the case of methanol the hydrogenation rate is unchanged after full activation of the catalyst (see Fig. 2). A change in the reaction rate is expected because with each addition the volume of the reaction mixture is increasing about

1–2%. The change in the reaction rate should be in the same order of magnitude, but the change is higher and therefore a catalyst deactivation is indicated. Often a deactivation of the catalyst takes place by the formation of “rhodium black” but this was not the case in our experiments. A better explanation for the change in the reaction rate can be given when the polarities of the substrate and the product and their distribution within the microheterogeneous systems are taken into account. Due to the fact that the catalyst is embedded in the unpolar core of the micelles, the substrate concentration inside the micelles is important for the reaction rate. This concentration is given by the partition coefficient  $K_{\text{MW}}$  of the substrate between the micellar core and the surrounding water. For the product the partition coefficient is even higher than for the substrate because after hydrogenation of the double bond the molecule is more hydrophobic, so that the product accumulates inside the micelles and lower the substrate concentration therein causing a decreasing reaction rate. When the total amount of product and substrate together becomes higher than the solubilization capacity of the micelles the reaction mixture no longer appears homogenous and changes from transparent (one phase system) to turbid (two phase system). This was observed from run 5 to run 8 for the SDS system (Fig. 8).

### 3.3 Partitioning of reactants between micelles and water

For the development of a continuous process applying micellar solutions as reaction media, the knowledge of the partition coefficient between the micelles and the water phase is of great

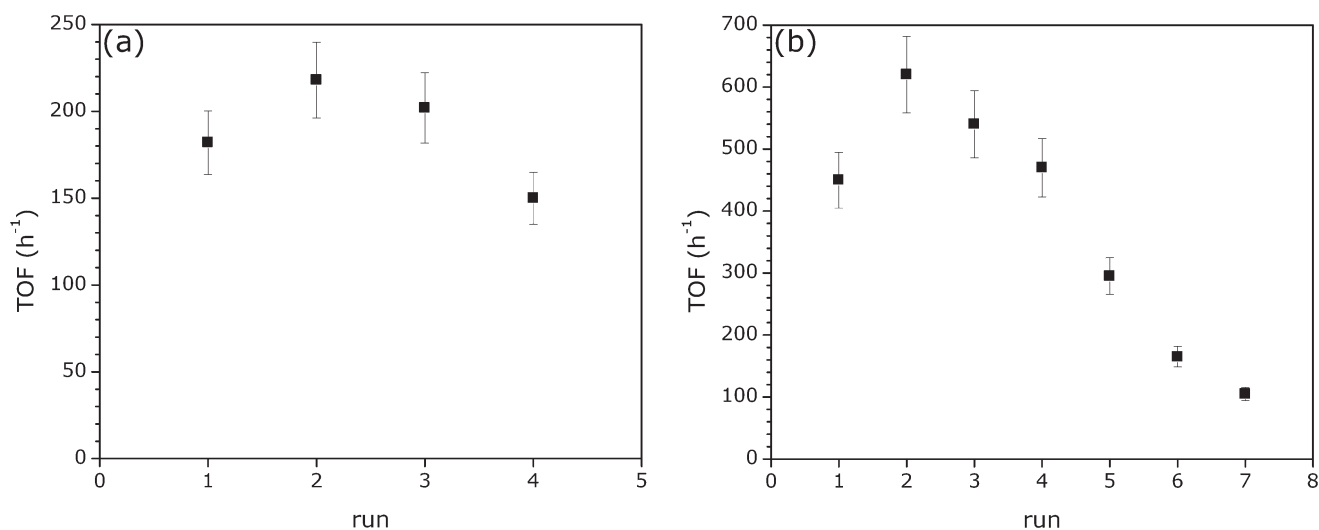


**Fig. 8** Repetitive batch hydrogenation of DMI in (a) Triton X-100 solution and (b) in SDS solution at 30 °C (Composition of a: 9.6 mmol TX-100, 64.1  $\mu\text{mol}$   $\text{Rh}(\text{cod})_2\text{CF}_3\text{SO}_3$ , 70.4  $\mu\text{mol}$  BPPM, 6.3 mmol DMI in each run,  $V = 105\text{--}108$  mL; Composition of b: 13.9 mmol SDS, 64.1  $\mu\text{mol}$   $\text{Rh}(\text{cod})_2\text{CF}_3\text{SO}_3$ , 70.4  $\mu\text{mol}$  BPPM, 12.6 mmol DMI in each run,  $V = 100\text{--}113$  mL). Error for TOF:  $\pm 10\%$ .

importance. During the reaction the partitioning of the reactants influences the reaction rate. Furthermore, the separation of the micellar and aqueous phase using an ultrafiltration membrane to isolate the product is mainly depending on the partition coefficient. While partition coefficients are well known for a lot of solutes (reactants) for two-phase systems like octanol/water, less information is given for aqueous micellar systems. Since partition coefficients cannot be measured in micellar solutions as simple as in liquid–liquid two phase systems, prediction of partition coefficients is highly useful. In this study the quantum chemical model COSMO-RS (Conductor-like Screening model for real solvents) is used for the prediction of partition coefficients for reactants and products of the hydrogenation (Table 4).

The partition coefficients for the Triton X-100 system have been verified by experimental data from ultrafiltration experiments. Additional information are given by Schwarze *et al.*<sup>41</sup> The increasing alkyl chain length of the different esters leads to higher hydrophobicity. Therefore the values of the partition coefficients increase with alkyl chain length. The values of the partition coefficients of the hydrogenated esters are even higher compared to those of the respective reactants, since the formed products are more hydrophobic. This leads to high product concentrations in the ultrafiltration retentate, what makes product isolation difficult. For itaconic acid and its hydrogenated product, the values of partition coefficients are nearly

the same. For all solutes partition coefficients  $K_{\text{MW}}$  in Triton X-100 solutions are higher compared to SDS solutions. This difference can be partially explained by the different micelle sizes (Table 1). The Triton X-100 micelles are larger and have a larger hydrophobic core. These larger hydrophobic cores accommodate a higher fraction of solute molecules in the solution than the smaller ones of SDS solutions. Such a behavior is most likely for non-polar solutes but in the case of ionic reactants which are dissolved in aqueous micellar solutions of ionic surfactants, ionic interactions can also play an important role and affect the partition coefficient. In order to show the influence of the partition coefficient of the substrate on the reaction rate, reaction rate profiles were modeled based on a simple Michaelis-Menten kinetic model (eqn (4)). In eqn (4),  $k_{\Phi}$  (catalyst concentration is included in  $k_{\Phi}$ ) and  $K_{\text{M}, \Phi}$  are the kinetic parameters for the reaction which takes place inside the micelles and  $\Phi$  is the micellar volume fraction of the solution. The concentration of the substrate  $[S_{\Phi}]$  in the micelles can be calculated from its total concentration  $[S]$  in the system using eqn (5). The partition coefficient  $P_{\text{MW}}$  ( $P_{\text{MW}} = [P_{\Phi}]/[P_{\text{W}}]$ ) is obtained from  $K_{\text{MW}}$  by eqn (6) in which  $v$  stands for the molar volumes.

$$\frac{d[S]}{dt} = -r_{\Phi} \cdot \Phi = k_{\Phi} \cdot \frac{[S_{\Phi}]}{[S_{\Phi}] + K_{\text{M}, \Phi}} \cdot \Phi \quad (4)$$

$$[S_{\Phi}] = \frac{[S]}{\left(\Phi + \frac{1}{P_{\text{MW}}} \cdot (1 - \Phi)\right)} \quad (5)$$

$$P_{\text{MW}} = K_{\text{MW}} \cdot \frac{v_{\text{Water}}}{v_{\text{Surfactant}}} \quad (6)$$

**Table 4** Partition coefficients for itaconates and their hydrogenation products for aqueous micellar TX-100 and SDS solutions predicted by COSMO-RS

	log $K_{\text{MW}}$ (TX-100)		log $K_{\text{MW}}$ (SDS)	
	Substrate	Product	Substrate	Product
IA (at pH 4)	2.2	2.5	1.6	2.0
DMI	2.3	2.8	2.3	2.6
DEI	3.0	3.4	2.8	3.1
DBI	5.2	5.7	4.3	4.8

For a set of estimated kinetic parameters, the reaction rate profiles for different partition coefficients are shown in Fig. 9.

It is obvious that with increasing  $P_{\text{MW}}$  the initial reaction rate increases and the total time to complete the reaction decreases. For  $P_{\text{MW}}$  values higher than 100 the reaction rate profile is not further affected. According to this approach the following order for the reaction rates in the hydrogenation reaction should be



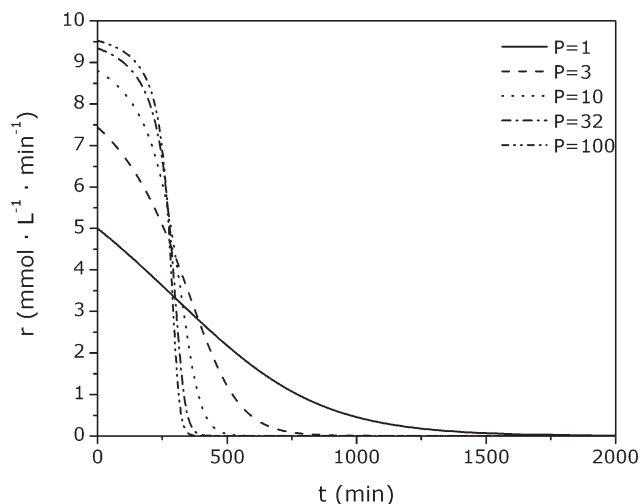


**Fig. 9** Reaction rate profiles for different partition coefficients:  $\Phi = 0.04$ ,  $k_{\Phi} = 10 \text{ mmol}/(\text{L} \cdot \text{min})$ ,  $K_{M, \Phi} = 100 \text{ mmol}/\text{L}$ ,  $c_S = 100 \text{ mmol}/\text{L}$ .

observed:  $r_{\text{DBI}} > r_{\text{DEI}} > r_{\text{DMI}} > r_{\text{IA}}$ . Unfortunately the intrinsic kinetic parameters change from substrate to substrate because of specific catalyst substrate interactions. If we compare the TOF values for the hydrogenation reactions of the different substrates with (*R,R*)-Et-FerroTane-Rhodium (Table 3: entries 4, 12, 16, and 18) we see that these interactions can overcompensate the effect of substrate partitioning. Additionally the formation of the product and its partitioning cannot be neglected. We assume that the formed product will also distribute between micelles and water and in case of a higher partition coefficient the substrate concentration in the micelles is lowered due to competitive partitioning. Here the exact function to include the formed product into the kinetic model of the reaction cannot be given.

#### 4. Integrated process

As shown in Scheme 1, an advantage of reactions in aqueous-micellar solutions is that the catalyst can be recycled by a subsequent membrane filtration step. For a successful integrated hydrogenation process, the separation step must be adjusted to the reaction. Here we showed results for an enantioselective hydrogenation reaction that was transferred from methanol to an aqueous micellar solution, and how it is affected by the choice of the surfactant and the surfactant concentration. In the best cases, this transfer happens with a decrease in activity but not in selectivity. The loss in activity can be compensated by a reuse of the catalyst, therefore the filtration step must be investigated. Here it is important to know which type of membrane, which surfactant concentration, and which operation mode have to be chosen for an optimal filtration step with respect to catalyst recovery and flux. In an earlier contribution<sup>20</sup> we found appropriate membranes for the filtration of aqueous-micellar SDS and TX-100 solutions, and we showed that the size of the membrane pores is one, but not the only parameter which controls the filtration process. It is obvious that the surfactant micelles should be bigger than the membrane pores to be retained, but, because of complex adsorption and diffusion interactions between the surfactant/micelles and the membrane surface, which lead not always to high retention data.

Furthermore we found that the surfactant concentration is one parameter which affects the flux dramatically. A detailed ultrafiltration study was performed with TX-100 at concentrations (20–80 g/L) able to solubilize a larger amount of hydrophobic solute.<sup>42</sup> At high surfactant concentrations, the flux is controlled by a gel-layer and becomes independent from the applied pressure difference. As a result, a low flux is obtained. Especially if the filtration is carried out in a *dead-end* analogue mode, the increasing surfactant concentration during the filtration will be problematic. In all integrated processes with step-wise catalyst recycling, the catalyst recovery was high, but the filtration times, in the same order than the reaction time, led to low space-time-yields.<sup>22</sup> Only an integrated process in which the reaction, the filtration, and the feeding of new reactants happen simultaneously, can overcome this problem. An example for the full continuous hydrogenation of DMI in aqueous-micellar TX-100 solution is shown in ref. 43. Beside the design of the ultrafiltration step by choosing the best operation conditions, one further parameter is of great importance: the substrate hydrophobicity. If the substrate is too hydrophobic, it will accumulate inside of the micelles and will be recycled to reactor together with the catalyst. Based on our results, we recommend the following conditions for aqueous-micellar solutions in an integrated process: (a) only hydrophilic substrates and hydrophobic catalysts should be used in combination, (b) the surfactant concentrations should be low and adjusted to the catalyst concentration, and (c) the integrated process should be carried out in a fully continuous mode.

#### 5. Conclusions

Aqueous micellar solutions are shown to be very useful alternative reaction media if appropriate surfactants are chosen which allow for a good performance of the catalyst characterized by an acceptable reaction rate and selectivity. In the best case the selectivity is in the same range as in methanol. The reaction rate is somewhat lower because of a lower hydrogen solubility in these systems. In some exceptional cases (*e.g.* Triton X-100) weak inhibition effects occur by unfavourable interactions of functional groups of the surfactant which compete with the substrate for the binding site of the catalyst. High TON (>1000) reached in repetitive batch runs show that no notable catalyst deactivation takes place in such media. The distribution of substrate and product within the microheterogeneous medium strongly affects both, reaction rate and product separation procedure. The better results should be obtained for more hydrophilic substrates that will not accumulate in the micelles. For more hydrophobic substrates a medium with a different structure, namely reverse micelles should be the better choice. With COSMO-RS we have a tool for tailoring the chemical nature of the surfactant according to our optimization criteria.

#### Acknowledgements

This work is part of the Cluster of Excellence “Unifying Concepts in Catalysis” coordinated by the Technische Universität Berlin. Financial support by the Deutsche Forschungsgemeinschaft (DFG) within the framework of the German Initiative for Excellence is gratefully acknowledged

(EXC 314). This part was also supported by the Deutsche Forschungsgemeinschaft (DFG) [SCHO 687/7-1] / [AR 236/32-1]. We thank Cognis for the donation of surfactant samples and Kornelia Gawlitza for DLS measurements.

## References

- H. Blaser, C. Malan, B. Pugin, F. Spindler, H. Steiner and M. Studer, *Adv. Synth. Catal.*, 2003, **345**, 103–151.
- J.A.F. Boogers, U. Felfer, M. Kotthaus, L. Lefort, G. Steinbauer, A.H.M. de Vries and J.G. de Vries, *Org. Process Res. Dev.*, 2007, **11**, 585–591.
- W. Knowles, *Adv. Synth. Catal.*, 2003, **345**, 3–13.
- H. Blaser, B. Pugin, F. Spindler and M. Thommen, *Acc. Chem. Res.*, 2007, **40**, 1240–1250.
- M. Roeper, *Chem. Unserer Zeit*, 2006, **40**, 126–135.
- D.J. Cole-Hamilton, *Science*, 2003, **299**, 1702–1706.
- B. Cornils, W.A. Herrmann, *Applied Homogeneous Catalysis with Organometallic Compounds*, Wiley-VCH, Weinheim, 2002.
- P. Wasserscheid and W. Keim, *Angew. Chem.*, 2000, **112**, 3926–3945.
- T. Welton, *Chem. Rev.*, 1999, **99**, 2071–2083.
- N.V. Plechkova and K.R. Seddon, *Chem. Soc. Rev.*, 2008, **37**, 123–150.
- W. Leitner, *Pure Appl. Chem.*, 2004, **76**, 635–644.
- D.E. Bergbreiter, *Chem. Rev.*, 2002, **102**, 3345–3384.
- R. van Heerbeek, P.C.J. Kamer, P.W.N.M. van Leeuwen and J.N.H. Reek, *Chem. Rev.*, 2002, **102**, 3717–3756.
- R.A. Sheldon, *Green Chem.*, 2008, **10**, 359–360.
- T. Dwars, E. Paetzold and G. Oehme, *Angew. Chem., Int. Ed.*, 2005, **44**, 7174–7199.
- G. Bianchini, A. Cavarzan, A. Scarso and G. Strukul, *Green Chem.*, 2009, **11**, 1517–1520.
- A. Cavarzan, A. Scarso and G. Strukul, *Green Chem.*, 2010, **12**, 790–794.
- L.-M. Wang, N. Jiao, J. Qiu, J.-J. Yu, J.-Q. Liu, F.-L. Guo and Y. Liu, *Tetrahedron*, 2010, **66**, 339–343.
- X.-H. Li, X.-G. Meng, Q.-H. Pang, S.-D. Liu, J.-M. Li, J. Du and C.-W. Hu, *J. Mol. Catal. A: Chem.*, 2010, **328**, 88–92.
- M. Schwarze, A. Rost, T. Weigel and R. Schomäcker, *Chem. Eng. Proc.*, 2009, **48**, 356–363.
- T. Dwars, J. Haberland, I. Grassert, G. Oehme and U. Kragl, *J. Mol. Catal. A: Chem.*, 2001, **168**, 81–86.
- J.S. Milano-Brusco, H. Nowothnick, M. Schwarze and R. Schomäcker, *Ind. Eng. Chem. Res.*, 2010, **49**, 1098–1104.
- T. Schmidt, Z. Dai, H. Drexler, W. Baummann, C. Jäger, D. Pfeifer and D. Heller, *Chem.–Eur. J.*, 2008, **14**, 4469–4471.
- T. Schmidt, H. Drexler, J. Sun, Z. Dai, W. Baummann, A. Preetz and D. Heller, *Adv. Synth. Catal.*, 2009, **351**, 750–754.
- J. Milano-Brusco, M. Schwarze, M. Djennad, H. Nowothnick and R. Schomäcker, *Ind. Eng. Chem. Res.*, 2008, **47**, 7586–7592.
- R. Benn and A. Ruffiniska, *Magn. Reson. Chem.*, 1988, **26**, 895–902.
- C.J. Elsevier, J.M. Ernsting and W.G.J. de Lange, *J. Chem. Soc., Chem. Commun.*, 1989, 585–586.
- M. Buggert, C. Cadena, L. Mokrushin, I. Smirnova, E.J. Maginn and W. Arlt, *Chem. Eng. Technol.*, 2009, **32**, 977–986.
- A. Klamt and F. Eckert, *Fluid Phase Equilib.*, 2000, **172**, 143.
- I. Benito, M.A. Garcia, C. Monge, J.M. Saz and M.L. Marina, *Colloids Surf., A*, 1997, **125**, 221–224.
- M. Kumbhakar, T. Goel, T. Mukherjee and H. Pal, *J. Phys. Chem. B*, 2004, **108**, 19246–19254.
- K. Streltzyk and G.D.J. Phillies, *Langmuir*, 1995, **11**, 42–47.
- N. Weitbrecht, M. Kratzat, S. Santoso and R. Schomäcker, *Catal. Today*, 2003, **79–80**, 401–408.
- T. Dwars and G. Oehme, *Adv. Synth. Catal.*, 2002, **344**, 239–260.
- U. Berens, M.J. Burk, A. Gerlach and W. Herts, *Angew. Chem., Int. Ed.*, 2000, **39**, 1981–1984.
- A. Preetz, H. Drexler, C. Fischer, Z. Dai, A. Börner, W. Baumann, A. Spannenberg, R. Thede and D. Heller, *Chem.–Eur. J.*, 2008, **14**, 1445–1451.
- D. Heller, S. Borns, W. Baumann and R. Selke, *Chem. Ber.*, 1996, **129**, 85–89.
- C.L. Young, *IUPAC Solubility Data Series, Volume 5/6: Hydrogen and Deuterium*, Pergamon Press, Oxford, New York, Toronto, Sydney, Paris, Frankfurt, 1981.
- H.-J. Drexler, A. Preetz, T. Schmidt, D. Heller, “Kinetics of homogeneous hydrogenations: measurements and interpretation”, chapter 11 in “Handbook of Homogeneous Hydrogenation” ed. by H. G. de Vries and C. Elsevier, 2007, 257–293.
- D. Heller, A. H. M. de Vries, J. G. de Vries, “Catalyst Inhibition and Deactivation in Homogeneous Hydrogenation”, chapter 44 in “Handbook of Homogeneous Hydrogenation” ed. by H. G. de Vries and C. Elsevier, 2007, 1483–1516.
- M. Schwarze, I. Volovych, S. Wille, L. Mokrushina, W. Arlt and R. Schomäcker, *Ind. Eng. Chem. Res.*, DOI: 10.1021/ie2006565doi.
- M. Schwarze, D. Le, S. Wille, A. Drews, W. Arlt and R. Schomäcker, *Sep. Purif. Technol.*, 2010, **74**, 21–27.
- R. Schomäcker, M. Schwarze, H. Nowothnick, A. Rost and T. Hamerla, *CIT*, DOI: 10.1002/cite.201100042.